

## Research Paper

# Naringenin-Loaded Nanoparticles Improve the Physicochemical Properties and the Hepatoprotective Effects of Naringenin in Orally-Administered Rats with CCl<sub>4</sub>-Induced Acute Liver Failure

Feng-Lin Yen,<sup>1</sup> Tzu-Hui Wu,<sup>1</sup> Liang-Tzung Lin,<sup>2</sup> Thau-Ming Cham,<sup>1,3</sup> and Chun-Ching Lin<sup>1,3</sup>

Received September 17, 2008; accepted November 7, 2008; published online November 25, 2008

**Purpose.** A novel naringenin-loaded nanoparticles system (NARN) was developed to resolve the restricted bioavailability of naringenin (NAR) and to enhance its hepatoprotective effects *in vivo* on oral administration.

**Materials and methods.** Physicochemical characterizations of NARN included assessment of particle size and morphology, powder X-ray diffraction, fourier transform infrared spectroscopy, and dissolution study. In addition, to evaluate its bioactivities and its oral treatment potential against liver injuries, we compared the hepatoprotective, antioxidant, and antiapoptotic effects of NARN and NAR on carbon tetrachloride (CCl<sub>4</sub>)-induced hepatotoxicity in rats.

**Results.** NARN had a significantly higher release rate than NAR and improved its solubility. NARN also exhibited more liver-protective effects compared to NAR with considerable reduction in liver function index and lipid peroxidation, in conjunction to a substantial increase in the levels of the antioxidant enzymes ( $P < 0.05$ ). Moreover, NARN was able to significantly inhibit the activation of caspase-3, -8, and -9 signaling, whereas NAR only markedly inhibited caspase-3 and -9 ( $P < 0.05$ ).

**Conclusion.** NARN effectively improved the release of NAR which resulted in more hepatoprotective effects mediated by its antioxidant and antiapoptotic properties. These observations also suggest that nanoformulation can improve the free drug's bioactivity on oral administration.

**KEY WORDS:** antiapoptotic; antioxidant; naringenin-loaded nanoparticles; oral administration; physicochemical characterization.

## INTRODUCTION

Oxidative stress contributes a decisive generating factor in the pathogenesis of acute and chronic liver diseases (1–3). Acute liver failure (ALF) is one of the acute liver diseases that can be caused by viruses, drugs, and toxins, and can lead to the development of hepatic encephalopathy and severe impairment of liver function (4). Carbon tetrachloride (CCl<sub>4</sub>) has been extensively used in animal models to explore chemical toxin-induced hepatic injury (5–7). The metabolism of CCl<sub>4</sub> catalyzed by liver microsomal cytochrome P450 rapidly overproduces free radicals that deplete hepatic glutathione and initiate a chain lipid peroxidation of the hepatocyte membrane. This ultimately results in the overproduction of reactive oxygen species (ROS) and hepatocyte injuries (8–10).

The toxic overproduction of ROS as superoxide anion (O<sub>2</sub><sup>•-</sup>), hydrogen peroxide (H<sub>2</sub>O<sub>2</sub>), and hydroxyl radicals (•OH) from the mitochondria are metabolized or scavenged by cellular enzymatic antioxidants including superoxide dismutase (SOD), catalase (CAT), and glutathione peroxidase (GPx) (11), or non-enzymatic antioxidants including vitamins (12) and flavonoids (13). The excessive mitochondrial ROS generation depletes the endogenous antioxidant enzymes and triggers hepatocyte apoptosis through activation of the caspases cascade, such as caspase-3, -8, and -9. Therefore, an external supply of antioxidants is essential to suppress caspase activation and for defense against the deleterious effects from oxidative stress (14–16).

Naringenin (4',5,7-trihydroxyflavanone, NAR; Fig. 1), a natural flavonoid aglycone of naringin, is widely distributed in citrus fruits (17), tomatoes (18), cherries (19), grapefruit (20), and cocoa (21). As a well-known antioxidant compound, the bioactivity of NAR has been attributed to its structure–activity relationship. The number of hydroxyl substitutions of NAR can donate hydrogen to ROS, allowing acquisition of stable structure, thus enabling scavenging of these free radicals (22,23). In addition, NAR has also been extensively investigated for its pharmacological activities, including anti-tumor (24), anti-inflammatory (25), and hepatoprotective (26) effects. Although NAR possesses excellent free radical

Feng-Lin Yen and Tzu-Hui Wu contributed equally to this work.

<sup>1</sup> Faculty of Pharmacy, College of Pharmacy, Kaohsiung Medical University, 100, Shih-Chuan 1st Road, Kaohsiung, 807, Taiwan.

<sup>2</sup> Department of Microbiology and Immunology, Dalhousie University, Halifax, Nova Scotia, Canada.

<sup>3</sup> To whom correspondence should be addressed. (e-mail: aalin@kmu.edu.tw)

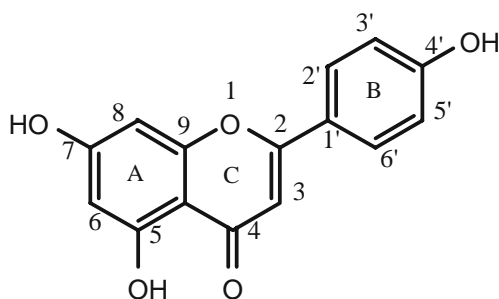


Fig. 1. Chemical structure of naringenin.

scavenging ability and pharmacological activities, clinical studies exploring different schedules of administration of this drug have been hampered by its extreme water insolubility. It has also been reported that the absolute bioavailability of NAR only achieved 4% in rabbits when the animals were orally administered (27). To overcome these obstacles, the delivery of NAR using novel dosage forms will likely yield more promising clinical applications of this compound.

Novel drug delivery systems (NDDS) can greatly improve the performance of drugs in terms of efficacy, solubility, and bioavailability (28). Particularly, nanoparticle system is one of the NDDS that is emerging as a highly promising technology in enhancing drug delivery. It has already been successfully used to improve the physicochemical profiles of drug compounds and increase their bioavailability (29). In the preparation of drug nanoparticles system, polymers are required for the immediate entrapment of the free compound and are used as carriers. The Eudragit® E (EE) cationic copolymer has been widely employed to improve solubility of poor water-soluble drugs (30). Because it possesses the basic site of dimethylamino groups which are ionized in the gastric fluid (31), this makes EE readily easy to dissolve in the gastric environment. Our previous study has demonstrated that the nanoparticle system of quercetin could be successfully developed using the Eudragit® E 100 polymer, and the antioxidant activities of the quercetin nanoparticles were observed to be more effective than the free pure drug (32).

The aim of the present study was to use a simple nanoprecipitation technique to develop a novel NAR-loaded nanoparticles (NARN) system and to evaluate its potential in improving the free drug's bioactivity on oral administration. The physicochemical characterization of NARN was determined by photon correlation spectroscopy (PCS), transmission electron microscopy (TEM), powder X-ray diffraction (XRD), and *in vitro* release. In addition, we assessed the liver functions influences, antioxidant effects, and the antiapoptotic activities from NARN in comparison to free-NAR to confirm its hepatoprotective mechanisms in CCl<sub>4</sub>-induced ALF and oxidative stress in rats. The hepatoprotective effects of NARN and free form NAR was determined by assessing levels of aspartate aminotransferase (AST) and alanine aminotransferase (ALT), and also by examining the histopathological sections of the liver, all of which are associated with hepatic integrity. Finally, the antioxidant and antiapoptotic mechanisms were explored by assessing changes in SOD, CAT, GPx, and malondialdehyde (MDA) levels, and measurements of the caspase-3, -8, and -9 activation, respectively.

## MATERIALS AND METHODS

### Materials

Naringenin (NAR), polyvinyl alcohol, Tris-HCl, thiobarbituric acid (TBA), ferrous chloride, ascorbate, dimethyl sulfoxide, polyvinyl alcohol, and ethylenediaminetetraacetic acid (EDTA) were purchased from Sigma-Aldrich Chemicals Co. (St. Louis, MO, USA). Aminoalkyl methacrylate copolymers (Eudragit® E) were obtained from Röhm Pharma (Dramstadt, Germany). All other chemical reagents were of analytical grade.

### Preparations of Naringenin Nanoparticles (NARN)

NARN system was prepared by the nanoprecipitation method (33,34). An amount of 50 mg of naringenin and an amount of 500 mg of Eudragit® E were dissolved in 25 ml of ethanol. The internal organic phase solutions were quickly injected into the 75 ml external aqueous solution containing 500 mg of PVA, and then the solutions were homogenized at 22,000 rpm for 25 min. The ethanol was completely removed by rotary vacuum evaporation at 40°C water bath and the remaining fraction was then lyophilized with a freeze dryer.

### Particle Size and Morphological Analysis of NARN

The mean particle size and polydispersity of NARN was determined by N5 submicron particle size analyzer (Beckman coulter, USA). NARN was diluted ten-fold with distilled water and subjected to analysis. Each value was measured in triplicate and the results are shown as mean  $\pm$  standard distribution. The morphology of NARN was also photographed by JEM-2000EXII instrument (JEOL Co. Tokyo, Japan).

### Reconstitution of Lyophilized NARN

Lyophilized NARN was reconstituted by addition of different pH buffer solutions (pH 1.2, 4.5, and 7.4, USPXXIV) or with purified water, followed by sonication in a water bath at room temperature for 5 min.

### X-Ray Diffractometry

The patterns of pure NAR and its lyophilized NARN were determined using the X-ray diffractometer (Siemens D5000, Germany). The scanned angle was set from  $2^\circ \leq 2\theta \leq 50^\circ$ , and the scanned rate was  $1^\circ/\text{min}$ .

### *In Vitro* Release Study

The concentration of NAR was analyzed by chromatographic system (Dionex P680). The analytical column used was the LichroCART® Purospher® STAR (250 $\times$ 4.6 mm i.d., 5  $\mu\text{m}$ ) and maintained at 37°C. The mobile phase was composed of 25 mM phosphate buffer and acetonitrile (50:50), and the pH value was adjusted to 2.5 with hydrochloric acid. The flow rate was set at 1.0 ml/min and the wavelength of UV detector was kept at 226 nm. *In vitro* studies of pure NAR and its nanoparticles were carried out in the simulated gastric fluid (USP XXIV) at  $37 \pm 0.5^\circ\text{C}$ . Samples

equivalent to 5 mg of NAR were placed in the 100 ml simulated gastric fluid which was stirred with a rotating paddle at 100 rpm. Then, 0.5 ml of each sample was withdrawn at time intervals of 5, 10, 20, 40, 60, 90, and 120 min, following which all samples were filtered with a 0.025  $\mu\text{m}$  filter (Millipore®). The concentration of the samples was determined by HPLC analysis.

### Design of CCl<sub>4</sub>-Induced Acute Liver Failure in Rats

Male Wistar-albino rats (4 weeks) were purchased from the National Laboratory Animal Center, Taiwan. They were housed in an air-conditioned room with temperature maintained at  $25\pm 1^\circ\text{C}$  and humidity at  $55\pm 5\%$  under a regular 12:12 h light/dark cycle for 1 week prior to treatment. All animals were fed the standard rodent chow and water *ad libitum*. The rats weighting 180–200 g were used for CCl<sub>4</sub>-induced hepatotoxicity. All rats received humane care in accordance to the “Guide for the Care and Use of Laboratory Animals” (National Academies Press, Washington, DC, USA, 1996). The method of acute hepatotoxicity induction followed that of Muriel and Mourelle with some modifications (35). Rats were randomly divided into four groups of five rats each. Normal control rats and CCl<sub>4</sub>-intoxicated hepatotoxicity group were orally treated by gavage using a gastric tube with distilled water for three consecutive days. For oral administration of the drugs, the NAR group was treated with NAR suspension in distilled water with Tween 20 (1%, *v/v*) at a dose of 100 mg/kg/day, and the NARN group was treated with NARN at a dose of 100 mg/kg/day, both for three consecutive days by gavage. On day 4, only the normal control group was intraperitoneally treated with 3 ml/kg isotonic 0.9% sodium chloride, and all other groups were intraperitoneally administered with a single dose of 3 ml/kg in 50% CCl<sub>4</sub> (olive oil:CCl<sub>4</sub>, 1:1). The rats were then sacrificed 24 h after CCl<sub>4</sub>-induced intoxication treatment. The blood was collected by cardiac puncture in glass tubes. The liver was immediately taken out and washed with ice-cold saline, then weighed and stored at  $-80^\circ\text{C}$ . The blood and liver samples were assessed for their biochemical, histological, and antioxidant changes.

### Evaluation of Serum AST and ALT Levels

The blood was centrifuged at 3,000 rpm at  $4^\circ\text{C}$  for 10 min to separate the serum. The aspartate aminotransferase (AST) and alanine aminotransferase (ALT) levels in the serum were measured with an auto-analyzer (Hitachi 7050, Tokyo, Japan).

### Measurement of Antioxidant Enzymes and Lipid Peroxidation

Liver tissues were homogenized in four volumes of ice-cold 150 mM Tris-HCl (pH 7.4) using a polytron homogenizer (Kinematica, Switzerland). The homogenates were centrifuged at  $1,600\times g$  for 15 min at  $4^\circ\text{C}$  to obtain a supernatant for various biochemical analyses. Lipid peroxidation in the liver homogenate was determined by the formation of MDA and measured by the thiobarbituric acid reactive method according to Ohkawa *et al.* (36). The SOD and GPx of liver homogenate activity was determined with a spectrophotometric

commercial SOD assay kit (Fluka) and glutathione peroxidase kit, respectively. CAT activity was assayed by measuring the exponential disappearance of H<sub>2</sub>O<sub>2</sub> (37). The protein concentration was measured by the method of Lowry *et al.* (38).

### Measurement of Caspases-3, -8, and -9 Activities

Caspases activity was determined using a colorimetric ELISA from R & D kit according to the manufacturer's protocol. Fresh liver tissues were homogenized in lysis buffer containing 100 mM HEPES buffer (pH 7.4), 20% glycerol, 10 mM dithiothreitol, and protease inhibitor, and subsequently the homogenates were centrifuged at  $15,000\times g$  for 20 min at  $4^\circ\text{C}$ . Supernatants were used for the determination of caspases activities by incubation at  $37^\circ\text{C}$  for 1 h and then measuring the absorbance by a spectrophotometer at 405 nm. Caspases activity was expressed as % relative to the control.

### Statistical Analysis

The results are presented as mean  $\pm$  standard deviation. Statistical analyses were conducted using one-way analysis of variance (ANOVA) with LSD by SPSS software, version 13 for Windows (SPSS, Inc., Chicago, IL, USA). A value of  $P < 0.05$  was considered to be statistically significant.

## RESULTS

### Physicochemical Characterization of NARN

The mean particle diameter of NARN was  $66.2\pm 0.38$  nm and its polydispersity was  $0.29\pm 0.04$  (Fig. 2A). The same finding was also observed from the TEM analysis of NARN which depicts its size in small spherical shape with uniform distribution (Fig. 2B). As shown in Fig. 3, the mean particle size of the lyophilized NARN was less than 65 nm when reconstituted in buffered solution of pH 1.2 and 4.5 (both presenting a clear solution) but not at pH 7.4 or in pure water ( $457.10\pm 18.49$  and  $369.57\pm 18.11$  nm, respectively; both presenting a turbid solution). These observations suggest that the particle size released can depend on the pH of the buffer solution. An explanation for this is that the low pH value could more easily dissolve the gastro-soluble Eudragit® E100 polymer from NARN, and thus yielded a more reduced particle size of NAR that is released.

The status of incorporated drug in nanoparticle system is an important factor that influences the solubility and bioavailability of the drug (39). Fig. 4 displays the XRD result of NAR and of its nanoparticles. The characteristic peaks of NAR presented clearly at a diffraction angle of  $2\theta$ ,  $10.73^\circ$ ,  $12.33^\circ$ ,  $15.87^\circ$ ,  $24.41^\circ$ ,  $26.50^\circ$ , and  $27.40^\circ$ , which could be inferred to traits of a highly crystalline structure. On the contrary, none of these characteristic peaks were present in the pattern of NARN suggesting that the crystal structure of NAR was indeed transformed into an amorphous state in NARN.

### Drug Release of NAR and NARN

Fig. 5 indicates the release of NAR and its nanoparticles NARN in simulated gastric medium. The release of the free

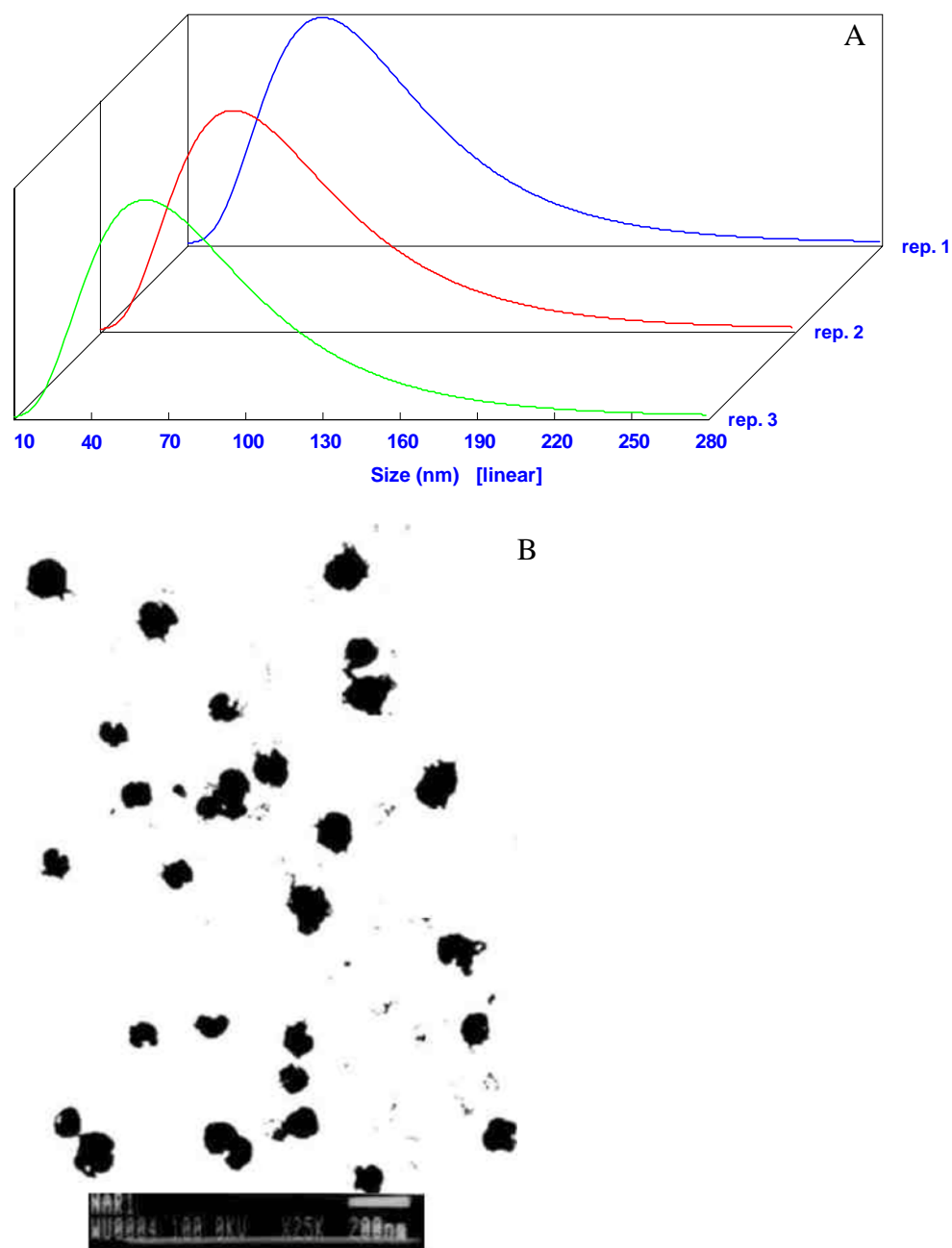


Fig. 2. Particles size distribution (A) and TEM photograph (B) of naringenin nanoparticles.

drug was less than 25% within 120 min. In contrast, NAR from the nanoparticle system dissolved more than 95% within 20 min. In the case of the release rate, NAR and NARN conformed to the Higuchi equation and the correlation coefficient ranged from 0.90 to 0.98 as shown in Table I. The release rate of NAR from the nanoparticle system was increased two-fold compared with free form NAR.

#### Hepatic Function Markers of NAR and NARN in Acute Liver Injury

The liver function markers in normal control, hepatotoxicity control, and treatment groups are shown in Fig. 6. The elevation of the serum AST (Fig. 6A) and ALT (Fig. 6B) levels in CCL<sub>4</sub>-intoxicated group was higher than the normal control

Table I. Release Rate Constants ( $K$ ) of NAR and the NARN System in the Simulated Gastric Fluid

	Higuchi equation	Correlation coefficient, $r$	$K$ ( $\text{min}^{-1/2}$ )
NAR	$y = 2.4728x - 0.4049$	0.9829	2.4728
NARN	$y = 5.2514x - 0.8003$	0.9030	5.2514

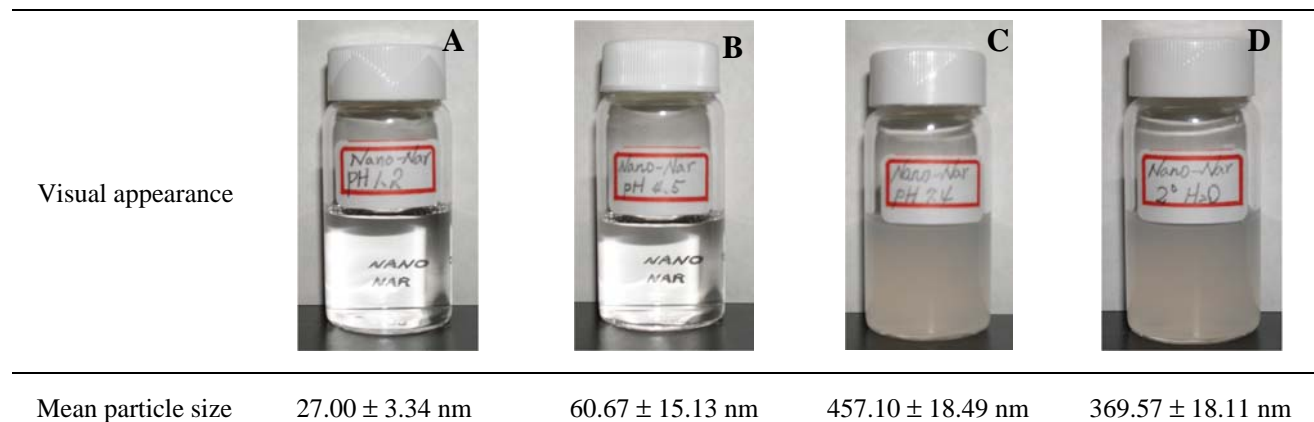


**Fig. 3.** Appearance and mean particle size of lyophilized NARN reconstituted in pH 1.2 (A), pH 4.5 (B), and pH 7.4 (C) solutions, and in pure water (D).

( $P < 0.05$ ). Pretreatment of ALF rats with NAR and its nanoparticles significantly reduced the liver function markers when compared with the  $\text{CCl}_4$ -intoxicated group ( $P < 0.05$ ). Further, we also found that the AST and ALT levels of NARN were two and 1.5-fold lower than NAR, respectively.

#### Effects of NAR and NARN on Hepatic Antioxidant Enzymes and Lipid Peroxidation

To understand the mechanisms of the antioxidant effect from NAR, we determined hepatic SOD, GPx, and CAT levels in ALF rats. As indicated in Fig. 7, the activities of the SOD (Fig. 7A), CAT (Fig. 7B), and GPx (Fig. 7C) levels in  $\text{CCl}_4$ -intoxicated groups were substantially reduced when compared with the normal control group ( $P < 0.05$ ). Pretreatment of the  $\text{CCl}_4$ -intoxicated acute liver injury rats with NAR or NARN however significantly raised the antioxidant activities levels ( $P < 0.05$ ). Interestingly, we also found that the SOD, CAT, and GPx levels from NARN treatment were 2.3, 2.0, and 2.1-fold superior to free form NAR, respectively. To assess lipid peroxidation in the liver, which is an estimate of free radical injury on the hepatic membrane, the MDA

levels were measured (20). Our results indicated that the level of MDA in  $\text{CCl}_4$ -intoxicated group was considerably increased compared with that of the normal control ( $P < 0.05$ ) (Fig. 7D). When the rats in the hepatic injury group were pretreated with NARN, the MDA levels were significantly reduced and were two-fold lower than NAR-pretreatment in the  $\text{CCl}_4$ -intoxicated group ( $P < 0.05$ ).

#### Effects on Hepatic Caspases Activity

The levels of caspase-3, -8, and -9 have been reported to play an important role in hepatocyte apoptosis (40,41). An elevation in caspase-3, -8, and -9 levels was observed in  $\text{CCl}_4$ -intoxicated ALF rats compared with the normal control animals ( $P < 0.05$ ) (Fig. 8). The  $\text{CCl}_4$  group pretreated with NAR had a significant suppression on the activation of caspase-3 and -9, but not on caspase-8. At the same dosage however, NARN could suppress all three caspases signaling activation when compared with the  $\text{CCl}_4$ -intoxicated ALF group ( $P < 0.05$ ).

## DISCUSSION

In the present study, we have successfully developed a novel naringenin-loaded nanoparticles (NARN) delivery system using Eudragit® E and polyvinyl alcohol as carriers by a simple nanoprecipitation technique. Our data suggested that the nanoparticles delivery system could considerably improve the physicochemical profile of naringenin and resulted in an increased drug release. In addition, NARN presented better hepatoprotective effects than NAR on oral administration through enhancement of its antioxidant and antiapoptotic activities in the  $\text{CCl}_4$ -induced hepatotoxicity rat model.

The nanoprecipitation technique possesses numerous advantages, being relatively straightforward and rapid, and offer reproducible particle size with a narrow distribution (33,42). Several literatures have established that the nanoparticles delivery system could substantially transform the original physicochemical properties of drugs and greatly improve its poor bioavailability (28,29). We have demonstrated that NARN has successfully changed several original

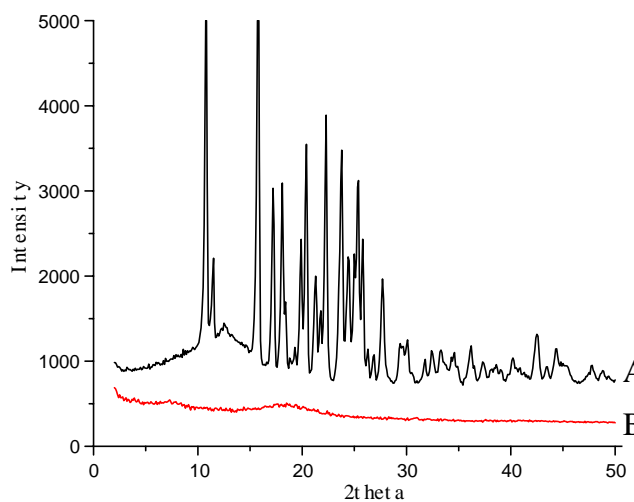


**Fig. 4.** X-ray diffraction patterns of free naringenin (A) and naringenin nanoparticles (B).

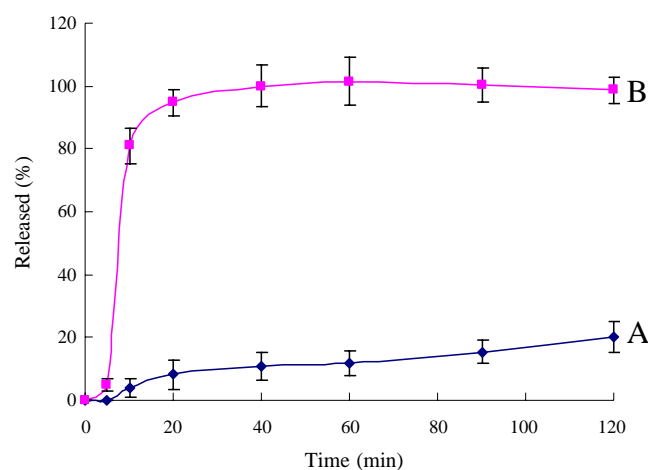


**Fig. 5.** Drug release profiles of free naringenin (A) and naringenin nanoparticles (B).

physicochemical properties of naringenin, including a reduction in particle size, the amorphous rendering of the crystalline structure, and an enhancement in drug release rate due to several reasons. First, in the process of nanoparticles preparation, NAR and EE have the same hydrophobic property, thus when blended together in the alcohol organic solvent, this generated a stronger affinity between them. In addition, PVA is an emulsion stabilizer that has been often used to stabilize nanoparticle systems (43). The hydrophilic and hydrophobic portion of PVA can interpenetrate into NAR-EE during the nanoprecipitation process to finally form a stable nanoparticle delivery system. Second, the result of the x-ray powder diffraction analysis displayed that NARN has an amorphous pattern lacking crystalline peaks seen in NAR. One explanation for this is that the molecules of NAR have been dispersed into the carriers thus rendering the clustered crystalline structure amorphous, an event similar to that observed in verteporfin-loaded nanoparticles (44). Finally, the release rate of NAR from the nanoparticle system was two-fold higher compared with the pure drug. The release mechanisms of NARN could be attributed to the reduction in drug particles size and the formation of the high-energy amorphous state. A similar finding has also been reported for quercetin nanoparticles in our previous study (32).

We have also observed that the near complete release of NAR from the nanoparticles system could be achieved at pH 1.2 within 20 min. This could be attributed to the reduction of drug particle size, the formation of drug high-energy amorphous state, the hydrophilic property of the Eudragit E polymer, and the enhanced wettability at acidic pH provided by the dissolved Eudragit E. A similar observation has been reported by Shah *et al.* (45). Our findings also suggest that in the experimental animals, pure NAR from the nanoparticle system was released through dissolution of the gastro-soluble Eudragit E100 polymer in the highly acidic environment of the stomach, and the released nanoparticulate form of the pure naringenin is what is responsible for the pharmacological activities of NARN observed *in vivo*. The gastric solubility profile of Eudragit E100 polymer was thus favorable to NARN in attaining optimal release of NAR which subsequently resulted in enhanced bioactive efficacy.

Aiming at preventing liver injury using NAR and its nanoparticles, we adopted the animal model of CCl<sub>4</sub>-induced ALF rats to investigate the hepatoprotective functions and the antioxidant mechanisms involved. CCl<sub>4</sub> is a classically known hepatotoxic compound that is metabolized and catalyzed by liver microsomal cytochrome P450 to trichloromethyl radical ( $\cdot\text{CCl}_3$ ) which then expeditiously reacts with oxygen to trichloromethyl peroxy radical ( $\cdot\text{CCl}_3\text{-O}_2\cdot$ ) in the liver cell (46). Meanwhile, ROS and lipid peroxides are overproduced during CCl<sub>4</sub> metabolism. In normal cellular environment, regular formation of ROS from the mitochondria are metabolized or scavenged by the cellular enzymatic antioxidants including SOD, CAT, and GPx. Intoxication with CCl<sub>4</sub> not only overproduces the ROS to exhaust cellular SOD, CAT, and GPx (47,48), but also results in ROS attacks on unsaturated fatty acids of phospholipids in the hepatocyte membrane to subsequently begin a chain reaction of lipid peroxidation (8,10). The ensuing oxidative stress from CCl<sub>4</sub>-intoxication could disrupt the structural integrity of the hepatic cell membrane and lead to leakage of AST and

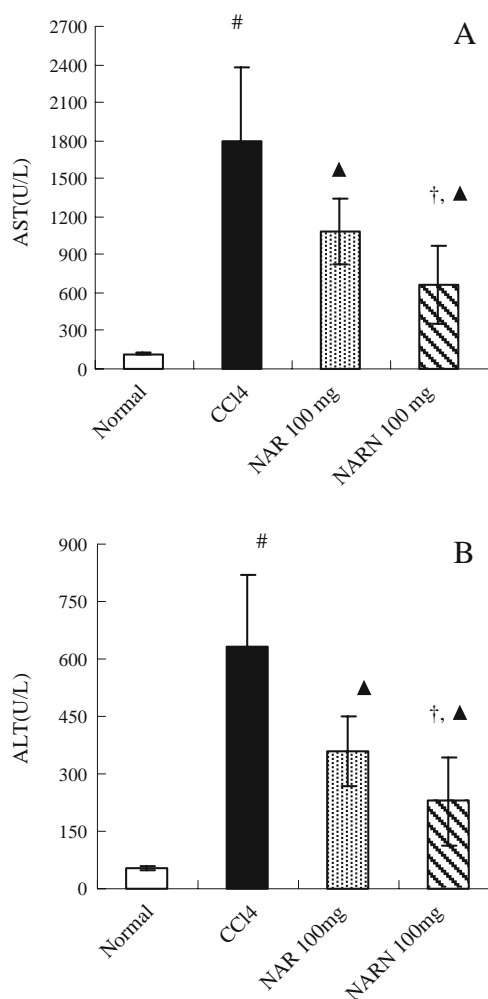


**Fig. 6.** Levels of liver function markers, AST (A) and ALT (B), from treatment with naringenin or its nanoparticles in CCl<sub>4</sub>-induced acute liver failure. Values were expressed as mean  $\pm$  S.D.,  $n=5$ . <sup>#</sup>Significantly different from the control ( $P<0.05$ ). <sup>▲</sup>Significantly different compared with the CCl<sub>4</sub>-intoxicated group ( $P<0.05$ ). <sup>†</sup>Significantly different compared with free form NAR treatment ( $P<0.05$ ).

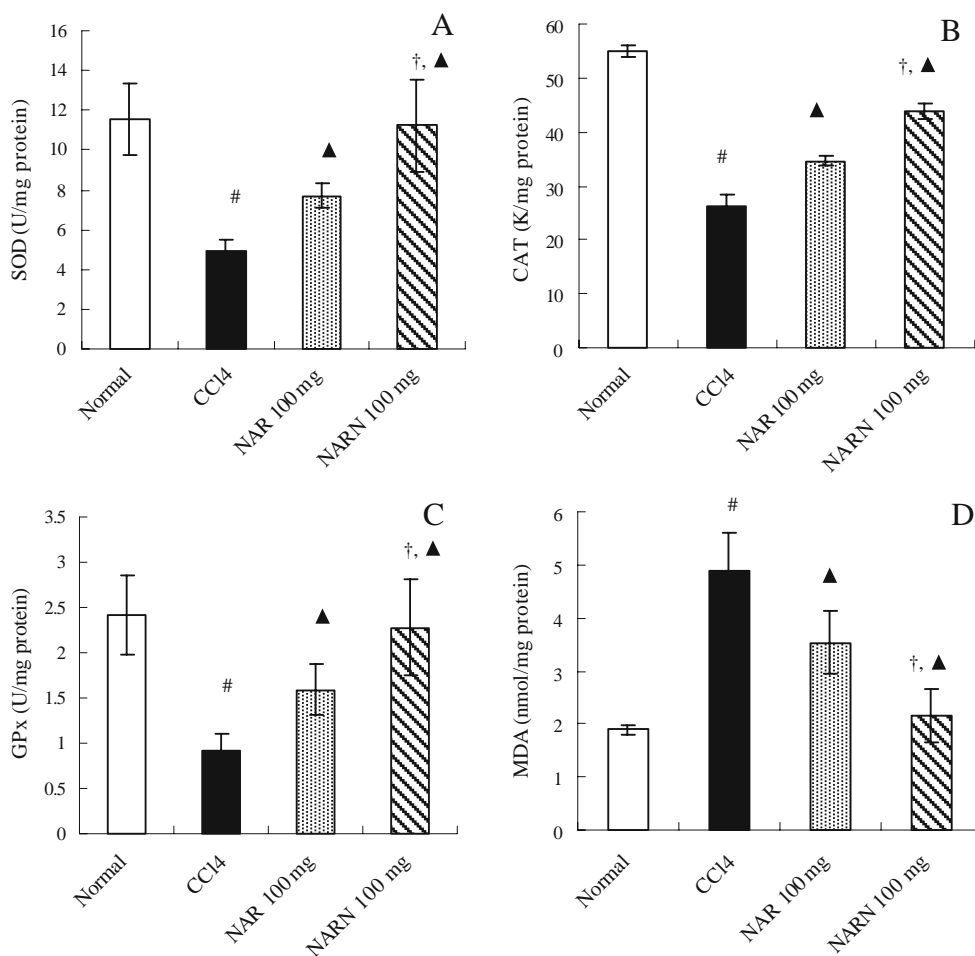


**Fig. 7.** Effect of free form naringenin (NAR) and its nanoparticles (NARN) on antioxidant enzyme activities, SOD (A), CAT (B), and GPx (C), and on lipid peroxidation, MDA (D), from liver homogenate in acute liver failure rats induced by CCl<sub>4</sub>. Values were expressed as mean  $\pm$  S.D., n=5. #Significantly different from the control ( $P<0.05$ ). ▲Significantly different compared with the CCl<sub>4</sub>-intoxicated group ( $P<0.05$ ). † Significantly different compared with free form NAR treatment ( $P<0.05$ ).

ALT hepatic cellular enzymes into the blood from dead hepatocytes, thus producing signs of hepatotoxicity (49,50).

Several studies have demonstrated that antioxidant supplements may be an excellent prevention strategy for many diseases, including liver injury, liver fibrosis, aging, cancer, and diabetes (51). Our results supported this notion in which NARN and NAR effectively prevented the CCl<sub>4</sub>-induced hepatotoxicity through antioxidant activities. In the CCl<sub>4</sub>-induced ALF animal model, both NAR and its nanoparticles counterpart played detoxifying roles in metabolizing the xenobiotics through enhancement of SOD, CAT, and GPx levels to scavenge the overproduction of ROS such as superoxide anions, hydrogen peroxide, and hydroxyl radicals generated from CCl<sub>4</sub>-intoxication. Consequently, by interfering with production of these initial ROS reactants in the chain reaction of lipid peroxidation, NAR and its nanoparticles were also able to diminish the MDA levels, and thereby prevent the cell membrane breakdown from the surplus of ROS. At the same time, our data also suggested that pretreatment with NAR and NARN effectively reduced the leakage of AST and ALT from hepatocytes necrosis, and prevented the CCl<sub>4</sub>-intoxication-mediated progression of hepatotoxicity, an effect likely owing to the above described

antioxidant activities. These effects are also confirmed in histopathological observations where considerably less signs of liver injuries were observed in liver sections from treatment mice (data not shown).

Comparing NAR and its nanoparticles, NARN exhibited greater effects in bioactivities and achieved higher potency than the free drug form *in vivo* upon oral treatment to the experimental animals. The nanoparticles size is a crucial factor for uptake into pathologic and inflamed tissues by macrophages and also for delivery drug across the fenestrated of the liver sinusoid (52,53). Previous studies have shown that macrophages from the bloodstream are activated and entered the injured liver during ALF (54), and phagocytosis mediated by macrophages can efficiently result in uptake of nanoparticle drugs into pathologic tissue and accumulate in the desired area (55). It has also been reported that particles-loaded drugs with a diameter of less than 200 nm reach the parenchymal cell of the liver easier and generate higher efficacy (53,56). Moreover, due to the improved aqueous solubility profile with the nanoparticles system, a high concentration of the bioactive compound could be delivered into the circulation. These properties of nanoparticles can explain why NARN having a smaller size (70 nm) and a

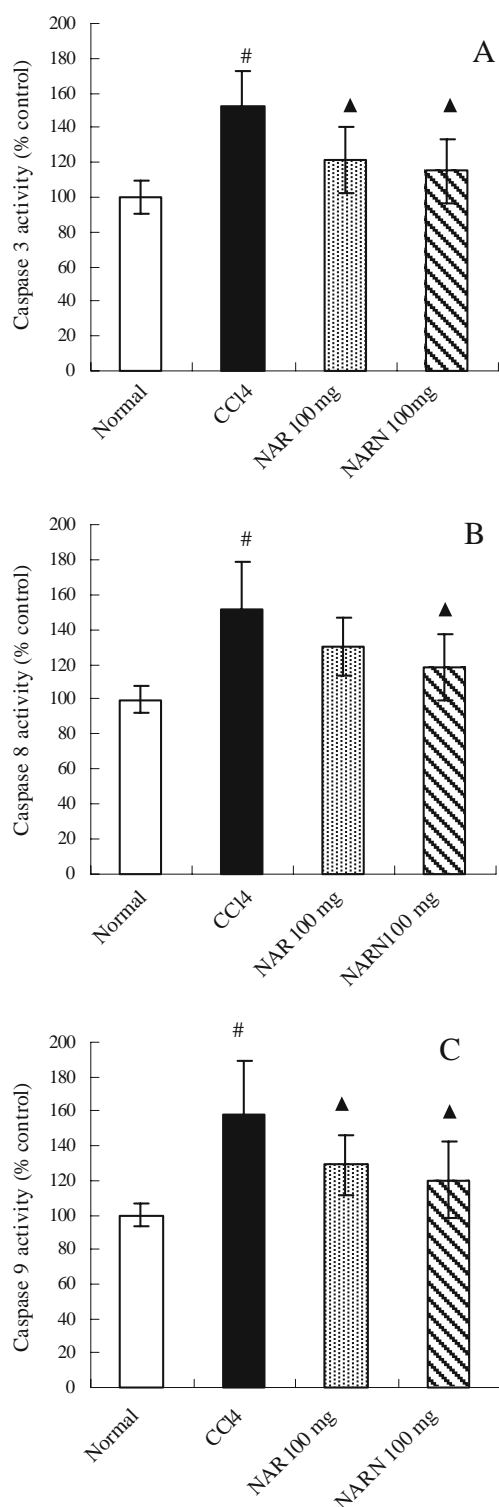


**Fig. 8.** Effect of free form naringenin (*NAR*) and its nanoparticles (*NARN*) on cytosolic caspase-3 (**A**), caspase-8 (**B**), and caspase-9 (**C**) activities from hepatocytes of CCl<sub>4</sub>-induced acute liver failure rats. Values were expressed as mean  $\pm$  S.D.,  $n=5$ . <sup>#</sup>Significantly different from the control ( $P<0.05$ ). <sup>^</sup>Significantly different compared with the CCl<sub>4</sub>-intoxicated group ( $P<0.05$ ).

better water solubility characteristic than the free drug yielded higher efficacy. The superiority of NARN over the free drug on its pharmacological activity is thus likely due to its smaller size resulting in easier uptake into pathologic liver tissues and facilitating its transport across the fenestrate of the liver sinusoid. Our *in vivo* data supported these ideas where NARN repeatedly outperformed NAR in its bioactivities, suggesting that the nanoparticulate system potentially offers enhancement in the pharmacological properties of the free drug on oral dosage.

CCl<sub>4</sub>-intoxication has been suggested to cause severe oxidative stress and apoptosis (49,57). Consequences from the toxin-induced excessive oxidative stress, depletion of antioxidant enzymes, and induction of membrane lipid peroxidation may prompt the extrinsic or intrinsic apoptotic pathways (58,59). Extrinsic pathway for apoptosis can be triggered by interaction of death receptors with ligands that leads to activation of caspases-8; intrinsic pathway for apoptosis is triggered by disruption of the mitochondrial membrane that leads to the activation of caspases-9 and subsequently followed by caspase-3 activation (60). Once triggered, the activation of caspase cascade initiates cell apoptosis that could cleave and inactivate plasma membrane Ca<sup>2+</sup> transport systems to induce cell membrane lysis and also secondary necrosis such as in CCl<sub>4</sub>-induced hepatotoxicity (61,62). Our data indicated that CCl<sub>4</sub> participates in the activation of the caspases to induce apoptosis of hepatocytes. Inhibiting the activation of apoptosis could therefore help prevent cell death and organ injury. Previous study has indicated that NAR protects human keratinocytes against UVB-induced apoptosis to decrease skin aging and cancer through its antiapoptotic and anti-lipid peroxidation effects (63). In our experiments, pretreatment with NARN significantly inhibited the activation of the caspase-3, -8, and -9 to prevent the hepatocyte from undergoing apoptosis. In contrast, NAR only showed inhibitory effects on caspase-3 and -9 whereas its effect on caspase-8 activation was less significant. As explained previously, it can be assumed that NARN being much more aqueous soluble than free NAR alone could help deliver a higher concentration of nanoparticulated NAR *in vivo*, and thus achieving a more potent inhibition on the caspase signaling cascades to prevent hepatocyte apoptosis. Therefore, NARN could more effectively suppress activation of the caspases than the free form NAR against CCl<sub>4</sub>-intoxication. Besides its effect in protecting the cells from caspase-triggered cell death program, the superior antioxidant and anti-lipid peroxidation activities from NARN compared with the free form NAR probably also helped in reducing cell necrosis, and further decreased secondary necrosis from triggering hepatocyte apoptosis. We suggest that the inhibition of ROS toxicity by NARN could be effective in preventing apoptosis activation by caspase cascades triggered through CCl<sub>4</sub>-induced hepatotoxicity.

In conclusion, the novel NAR-loaded nanoparticles delivery system developed in this study helped enhance the free drug's hepatoprotective, antioxidant, and antiapoptotic effects in ameliorating CCl<sub>4</sub> toxicity-triggered necrosis and apoptosis. These findings also proved that the particle size was an important factor for acquiring optimal *in vivo* efficacy, and that nanoparticles could be used to improve the



bioavailability of NAR on oral administration. Finally, we suggest that NARN merits further investigation for clinical application such as in prophylaxis of chronic liver diseases.

## ACKNOWLEDGEMENTS

The authors would like to thank Mrs. Shui-Chin Lu (Department of Medical Research, Kaohsiung Medical University) for technical support with the TEM. This study was supported by a research grant from the National Science Council of Taiwan (NSC 97-2313-B-037-001-MY3).

## REFERENCES

- K. Tanikawa, and T. Torimura. Studies on oxidative stress in liver diseases: important future trends in liver research. *Med. Mol. Morphol.* **39**:22 (2006). doi:10.1007/s00795-006-0313-z.
- L. Cesaratto, C. Vascotto, S. Calligaris, and G. Tell. The importance of redox state in liver damage. *Ann. Hepatol.* **3**:86 (2004).
- D. J. Tuma. Role of malondialdehyde-acetaldehyde adducts in liver injury. *Free. Radic. Biol. Med.* **32**:303 (2002). doi:10.1016/S0891-5849(01)00742-0.
- R. Q. Gill, and R. K. Sterling. Acute liver failure. *J. Clin. Gastroenterol.* **33**:191 (2001). doi:10.1097/00004836-200109000-00005.
- S. R. Naik, and V. S. Panda. Antioxidant and hepatoprotective effects of *Ginkgo biloba* phytosomes in carbon tetrachloride-induced liver injury in rodents. *Liver. Int.* **27**:393 (2007). doi:10.1111/j.1478-3231.2007.01463.x.
- C. P. Lee, P. H. Shih, C. L. Hsu, and G. C. Yen. Hepatoprotection of tea seed oil (*Camellia oleifera* Abel.) against CCl<sub>4</sub>-induced oxidative damage in rats. *Food. Chem. Toxicol.* **45**:888 (2007). doi:10.1016/j.fct.2006.11.007.
- Z. M. Wu, T. Wen, Y. F. Tan, Y. Liu, F. Ren, and H. Wu. Effects of salvianolic acid A on oxidative stress and liver injury induced by carbon tetrachloride in rats. *Basic. Clin. Pharmacol. Toxicol.* **100**:115 (2007).
- L. W. Weber, M. Boll, and A. Stampfl. Hepatotoxicity and mechanism of action of haloalkanes: carbon tetrachloride as a toxicological model. *Crit. Rev. Toxicol.* **33**:105 (2003). doi:10.1080/713611034.
- G. Poli. Liver damage due to free radicals. *Br. Med. Bull.* **49**:604 (1993).
- S. Basu. Carbon tetrachloride-induced lipid peroxidation: eicosanoid formation and their regulation by antioxidant nutrients. *Toxicology.* **189**:113 (2003). doi:10.1016/S0300-483X(03)00157-4.
- P. Y. Chiu, M. H. Tang, D. H. Mak, M. K. Poon, and K. M. Ko. Hepatoprotective mechanism of schisandrin B: role of mitochondrial glutathione antioxidant status and heat shock proteins. *Free. Radic. Biol. Med.* **35**:368 (2003). doi:10.1016/S0891-5849(03)00274-0.
- U. Singh, S. Devaraj, and I. Jialal. Vitamin E, oxidative stress, and inflammation. *Annu. Rev. Nutr.* **25**:151 (2005). doi:10.1146/annurev.nutr.24.012003.132446.
- P. G. Pietta. Flavonoids as antioxidants. *J. Nat. Prod.* **63**:1035 (2000). doi:10.1021/np9904509.
- T. Ozben. Oxidative stress and apoptosis: impact on cancer therapy. *J. Pharm. Sci.* **96**:2181 (2007). doi:10.1002/jps.20874.
- H. Schulze-Bergkamen, M. Schuchmann, B. Fleischer, and P. R. Galle. The role of apoptosis versus oncotic necrosis in liver injury: facts or faith? *J. Hepatol.* **44**:984 (2006). doi:10.1016/j.jhep.2006.02.004.
- C. Garcia-Ruiz, and J. C. Fernández-Checa. Redox regulation of hepatocyte apoptosis. *J. Gastroenterol. Hepatol.* **22**(Suppl 1):S38 (2007). doi:10.1111/j.1440-1746.2006.04644.x.
- A. Dembinski, Z. Warzecha, S.J. Konturek, P. Ceranowicz, M. Dembinski, W. W. Pawlik, B. Kusnierz-Cabala, and J.W. Naskalski. Extract of grapefruit-seed reduces acute pancreatitis induced by ischemia/reperfusion in rats: possible implication of tissue antioxidants. *J. Physiol. Pharmacol.* **55**:811 (2004).
- G. Le Gall, M. S. DuPont, F. A. Mellon, A. L. Davis, G. J. Collins, M. E. Verhoeven, and I. J. Colquhoun. Characterization and content of flavonoid glycosides in genetically modified tomato (*Lycopersicon esculentum*) fruits. *J. Agric. Food. Chem.* **51**:2438 (2003). doi:10.1021/jf025995e.
- H. Wang, M. G. Nair, G. M. Strasburg, A. M. Booren, and J. I. Gray. Antioxidant polyphenols from tart cherries (*Prunus cerasus*). *J. Agric. Food. Chem.* **47**:840 (1999). doi:10.1021/jf980936f.
- I. Erlund, E. Meririnne, G. Alftan, and A. Aro. Plasma kinetics and urinary excretion of the flavanones naringenin and hesperetin in humans after ingestion of orange juice and grapefruit juice. *J. Nutr.* **131**:235 (2001).
- T. Stark, S. Bareuther, and T. Hofmann. Sensory-guided decomposition of roasted cocoa nibs (*Theobroma cacao*) and structure determination of taste-active polyphenols. *J. Agric. Food. Chem.* **53**:5407 (2005). doi:10.1021/jf050457y.
- S. C. Shen, C. H. Ko, S. W. Tseng, S. H. Tsai, and Y. C. Chen. Structurally related antitumor effects of flavanones *in vitro* and *in vivo*: involvement of caspase 3 activation, p21 gene expression, and reactive oxygen species production. *Toxicol. Appl. Pharmacol.* **197**:84 (2004). doi:10.1016/j.taap.2004.02.002.
- H. J. Heo, D. O. Kim, S. C. Shin, M. J. Kim, B. G. Kim, and D. H. Shin. Effect of antioxidant flavanone, naringenin, from *Citrus junoson* neuroprotection. *J. Agric. Food. Chem.* **52**:1520 (2004). doi:10.1021/jf035079g.
- S. Kanno, A. Tomizawa, T. Hiura, Y. Osanai, A. Shouji, M. Ujibe, T. Ohtake, K. Kimura, and M. Ishikawa. Inhibitory effects of naringenin on tumor growth in human cancer cell lines and sarcoma S-180-implanted mice. *Biol. Pharm. Bull.* **28**:527 (2005). doi:10.1248/bpb.28.527.
- S. Hirai, Y. I. Kim, T. Goto, M. S. Kang, M. Yoshimura, A. Obata, R. Yu, and T. Kawada. Inhibitory effect of naringenin chalcone on inflammatory changes in the interaction between adipocytes and macrophages. *Life. Sci.* **81**:1272 (2007). doi:10.1016/j.lfs.2007.09.001.
- M. H. Lee, S. Yoon, and J. O. Moon. The flavonoid naringenin inhibits dimethylnitrosamine-induced liver damage in rats. *Biol. Pharm. Bull.* **27**:72 (2004). doi:10.1248/bpb.27.72.
- S. L. Hsiu, T. Y. Huang, Y. C. Hou, D. H. Chin, and P. D. Chao. Comparison of metabolic pharmacokinetics of naringin and naringenin in rabbits. *Life. Sci.* **70**:1481 (2002). doi:10.1016/S0024-3205(01)01491-6.
- D. V. Ratnam, D. D. Ankola, V. Bhardwaj, D. K. Sahana, and M. N. Kumar. Role of antioxidants in prophylaxis and therapy: A pharmaceutical perspective. *J. Control. Release.* **113**:189 (2006). doi:10.1016/j.jconrel.2006.04.015.
- J. Dai, T. Nagai, X. Wang, T. Zhang, M. Meng, and Q. Zhang. pH-sensitive nanoparticles for improving the oral bioavailability of cyclosporine A. *Int. J. Pharm.* **280**:229 (2004). doi:10.1016/j.ijpharm.2004.05.006.
- J. Y. Jung, S. D. Yoo, S. H. Lee, K. H. Kim, D. S. Yoon, and K. H. Lee. Enhanced solubility and dissolution rate of itraconazole by a solid dispersion technique. *Int. J. Pharm.* **187**:209 (1999). doi:10.1016/S0378-5173(99)00191-X.
- S. L. Wang, S. Y. Lin, T. F. Chen, and W. T. Cheng. Eudragit E accelerated the diketopiperazine formation of enalapril maleate determined by thermal FTIR microspectroscopic technique. *Pharm. Res.* **21**:2127 (2004). doi:10.1023/B:PHAM.0000048206.62093.4e.
- T. H. Wu, F. L. Yen, L. T. Lin, T. R. Tsai, C. C. Lin, and T. M. Cham. Preparation, physicochemical characterization, and antioxidant effects of quercetin nanoparticles. *Int. J. Pharm.* **346**:160 (2008). doi:10.1016/j.ijpharm.2007.06.036.
- U. Bilati, E. Allémann, and E. Doelker. Nanoprecipitation versus emulsion-based techniques for the encapsulation of proteins into biodegradable nanoparticles and process-related stability issues. *AAPS. PharmSciTech.* **6**:E594 (2005). doi:10.1208/pt060474.
- Z. Zili, S. Sfar, and H. Fessi. Preparation and characterization of poly-epsilon-caprolactone nanoparticles containing griseofulvin. *Int. J. Pharm.* **294**:261 (2005). doi:10.1016/j.ijpharm.2005.01.020.
- P. Muriel, and M. Mourelle. Characterization of membrane fraction lipid composition and function of cirrhotic rat liver.

- Role of S-adenosyl-L-methionine. *J. Hepatol.* **14**:16 (1992). doi:10.1016/0168-8278(92)90125-9.
36. H. Ohkawa, N. Ohishi, and K. Yagi. Assay for lipid peroxides in animal tissues by thiobarbituric acid reaction. *Anal. Biochem.* **95**:351 (1979). doi:10.1016/0003-2697(79)90738-3.
  37. H. Aebi. Catalase *in vitro*. *Methods Enzymol.* **105**:121 (1984). doi:10.1016/S0076-6879(84)05016-3.
  38. O. H. Lowry, N. J. Rosebrough, A. L. Farr, and R. J. Randall. Protein measurement with the Folin phenol reagent. *J. Biol. Chem.* **193**:265 (1951).
  39. J. Xing, D. Zhang, and T. Tan. Studies on the oridonin-loaded poly(D,L-lactic acid) nanoparticles *in vitro* and *in vivo*. *Int. J. Biol. Macromol.* **40**:153 (2007). doi:10.1016/j.ijbiomac.2006.07.001.
  40. T. Y. Lee, H. H. Chang, M. Y. Wu, and H. C. Lin. Yin-Chen-Hao-Tang ameliorates obstruction-induced hepatic apoptosis in rats. *J. Pharm. Pharmacol.* **59**:583 (2007). doi:10.1211/jpp.59.4.0014.
  41. T. Y. Lee, H. H. Chang, G. J. Wang, J. H. Chiu, Y. Y. Yang, and H. C. Lin. Water-soluble extract of *Salvia miltiorrhiza* ameliorates carbon tetrachloride-mediated hepatic apoptosis in rats. *J. Pharm. Pharmacol.* **58**:659 (2006). doi:10.1211/jpp.58.5.0011.
  42. Y. Chen, J. Liu, X. Yang, X. Zhao, and H. Xu. Oleonic acid nanosuspensions: preparation, *in-vitro* characterization and enhanced hepatoprotective effect. *J. Pharm. Pharmacol.* **57**:259 (2005). doi:10.1211/0022357055407.
  43. S. K. Sahoo, J. Panyam, S. Prabha, and V. Labhsetwar. Residual polyvinyl alcohol associated with poly (D,L-lactide-co-glycolide) nanoparticles affects their physical properties and cellular uptake. *J. Control. Release.* **82**:105 (2002). doi:10.1016/S0168-3659(02)00127-X.
  44. Y. N. Konan-Kouakou, R. Boch, R. Gurny, and E. Allemann. *In vitro* and *in vivo* activities of verteporfin-loaded nanoparticles. *J. Control. Release.* **103**:83 (2005). doi:10.1016/j.jconrel.2004.11.023.
  45. P. P. Shah, R. C. Mashru, Y. M. Rane, and A. Thakkar. Design and optimization of mefloquine hydrochloride microparticles for bitter taste masking. *AAPS. PharmSciTech.* **9**:377 (2008). doi:10.1208/s12249-008-9052-x.
  46. D. R. Koop. Oxidative and reductive metabolism by cytochrome P450 2E1. *FASEB. J.* **6**:724 (1992).
  47. C. Y. Wang, F. L. Ma, J. T. Liu, J. W. Tian, and F. H. Fu. Protective effect of salvianic acid A on acute liver injury induced by carbon tetrachloride in rats. *Biol. Pharm. Bull.* **30**:44 (2007). doi:10.1248/bpb.30.44.
  48. M. A. Mansour. Protective effects of thymoquinone and desferrioxamine against hepatotoxicity of carbon tetrachloride in mice. *Life. Sci.* **66**:2583 (2000). doi:10.1016/S0024-3205(00)00592-0.
  49. F. Sun, E. Hamagawa, C. Tsutsui, Y. Ono, Y. Ogiri, and S. Kojo. Evaluation of oxidative stress during apoptosis and necrosis caused by carbon tetrachloride in rat liver. *Biochim. Biophys. Acta.* **1535**:186 (2001).
  50. H. Ikeda, Y. Kume, K. Tejima, T. Tomiya, T. Nishikawa, N. Watanabe, N. Ohtomo, M. Arai, C. Arai, M. Omata, K. Fujiwara, and Y. Yatomi. Rho-kinase inhibitor prevents hepatocyte damage in acute liver injury induced by carbon tetrachloride in rats. *Am. J. Physiol. Gastrointest. Liver. Physiol.* **293**:G911 (2007). doi:10.1152/ajpgi.00210.2007.
  51. R. Rodrigo, C. Guichard, and R. Charles. Clinical pharmacology and therapeutic use of antioxidant vitamins. *Fundam. Clin. Pharmacol.* **21**:111 (2007). doi:10.1111/j.1472-8206.2006.00466.x.
  52. Y. Hu, J. Xie, Y. W. Tong, and C. H. Wang. Effect of PEG conformation and particle size on the cellular uptake efficiency of nanoparticles with the HepG2 cells. *J. Control. Release.* **118**:7 (2007). doi:10.1016/j.jconrel.2006.11.028.
  53. H. F. Liang, T. F. Yang, C. T. Huang, M. C. Chen, and H. W. Sung. Preparation of nanoparticles composed of poly(gamma-glutamic acid)-poly(lactide) block copolymers and evaluation of their uptake by HepG2 cells. *J. Control. Release.* **105**:213 (2005). doi:10.1016/j.jconrel.2005.03.021.
  54. A. Salazar-Montes, V. Delgado-Rizo, and J. Armenda-riz-Borunda. Differential gene expression of pro-inflammatory and anti-inflammatory cytokines in acute and chronic liver injury. *Hepatol. Res.* **16**:181 (2000). doi:10.1016/S1386-6346(99)00048-0.
  55. A. Lamprecht, N. Ubrich, H. Yamamoto, U. Schäfer, H. Takeuchi, P. Maincent, Y. Kawashima, and C.M. Lehr. Biodegradable nanoparticles for targeted drug delivery in treatment of inflammatory bowel disease. *J. Pharmacol. Exp. Ther.* **299**:775 (2001).
  56. M. Hashida, S. Takemura, M. Nishikawa, and Y. Takakura. Targeted delivery of plasmid DNA complexed with galactosylated poly(L-lysine). *J. Control. Release.* **53**:301 (1998). doi:10.1016/S0168-3659(97)00263-0.
  57. J. Shi, K. Aisaki, Y. Ikawa, and K. Wake. Evidence of hepatocyte apoptosis in rat liver after the administration of carbon tetrachloride. *Am. J. Pathol.* **153**:515 (1998).
  58. B. Zhang, J. Hirahashi, X. Cullere, and T. N. Mayadas. Elucidation of molecular events leading to neutrophil apoptosis following phagocytosis: cross-talk between caspase 8, reactive oxygen species, and MAPK/ERK activation. *J. Biol. Chem.* **278**:28443 (2003). doi:10.1074/jbc.M210727200.
  59. N. Kaplowitz. Biochemical and cellular mechanisms of toxic liver injury. *Semin. Liver. Dis.* **22**:137 (2002). doi:10.1055/s-2002-30100.
  60. M. L. Bajt, S.L. Vonderfecht, and H. Jaeschke. Differential protection with inhibitors of caspase-8 and caspase-3 in murine models of tumor necrosis factor and Fas receptor-mediated hepatocellular apoptosis. *Toxicol. Appl. Pharmacol.* **175**:243 (2001). doi:10.1006/taap.2001.9242.
  61. S. M. Riordan, and R. Williams. Mechanisms of hepatocyte injury, multiorgan failure, and prognostic criteria in acute liver failure. *Semin. Liver. Dis.* **23**:203 (2003). doi:10.1055/s-2003-42639.
  62. M. E. Guicciardi, and G. J. Gores. Apoptosis: a mechanism of acute and chronic liver injury. *Gut.* **54**:1024 (2005). doi:10.1136/gut.2004.053850.
  63. M. A. El-Mahdy, Q. Zhu, Q. E. Wang, G. Wani, S. Patnaik, Q. Zhao, E. S. Arafa, B. Barakat, S. N. Mir, and A. A. Wani. Naringenin protects HaCaT human keratinocytes against UVB-induced apoptosis and enhances the removal of cyclobutane pyrimidine dimers from the genome. *Photochem. Photobiol.* **84** (2):307-316 (2007).